Mission Analysis, Spacecraft Concept and Ion Thruster Design for a Low-Cost Rendezvous with an Asteroid

IEPC-2005-226

David G Fearn.[*]
EP Solutions, Fleet, Hampshire, GU52 6HS, UK

Abstract: **This paper summarises a study in which it is shown that a small spacecraft, with a launch mass of less than 200 kg, can accomplish a very challenging deep space mission. By using an innovative solar array and ion engines operating at high specific impulse (SI), a total velocity increment exceeding 12 km/s can be provided, which allows a rendezvous to be achieved with a very wide variety of asteroids, out to a distance from the sun of 2 AU. The paper includes an optimisation of the SI, the detailed design of a small ion engine satisfying the mission requirements, and a description of the solar array, which produces about 2 kW. With a launch mass of less than 200 kg, it is assumed that a low-cost auxiliary passenger launch to geostationary transfer orbit on an Ariane 5 will be employed.**

Nomenclature

A	=	grid area	m_i	=	ion mass
a	=	asteroid orbital semi-major axis	$\dot{m}_c$	=	hollow cathode flow rate
B	=	discharge chamber magnetic field	$\dot{m}_D$	=	flow rate to discharge chamber
D	=	asteroid diameter	$\dot{m}_T$	=	total propellant flow rate
d	=	ion acceleration distance	n_e	=	electron number density
e	=	asteroid orbital eccentricity	P_B	=	ion beam power
e	=	charge on an electron	P_D	=	total discharge chamber power
g_o	=	acceleration due to gravity at sea level	p_e	=	electron pressure in coupling plasma
			P_g	=	grid system perveance factor
I_A	=	anode current	P_N	=	neutraliser discharge power
I_B	=	ion beam current	P_T	=	total thruster input power
I_{sp}	=	specific impulse	p	=	asteroid orbital period
I^+	=	ion production rate	q	=	asteroid perihelion distance
I^-	=	primary electron current	R	=	radius of ion beam
i	=	asteroid orbital inclination	S	=	distance from cathode orifice to edge of inner polepiece
j_p	=	current density in annular gap around baffle disc	T	=	thrust
K	=	M_f/M_i	T_e	=	electron temperature
L	=	dominant length of discharge chamber	T_g	=	screen grid transparency
			V_A	=	anode potential
M_b	=	basic spacecraft mass, excluding propellant and tank	V_{ac}	=	accel grid potential
			V_B	=	net ion accelerating potential
M_i	=	spacecraft initial (launch) mass	V_k	=	keeper potential
M_f	=	spacecraft final (dry) mass	V_p	=	plasma potential

---

[*] Sole Proprietor; Senior Member of AIAA; dg.fearn@virgin.net.

Nomenclature (Cond)

V_T	=	total ion beam accelerating potential	ΔM =	propellant mass
α_t	=	tank structural support mass as fraction of propellant mass	ΔM_t =	mass of propellant plus tank plus support structure
α_t	=	tank mass as fraction of propellant mass	ΔV =	spacecraft velocity increment
			η_m =	propellant utilisation efficiency
ε_o	=	dielectric constant of free space		

I.   Introduction

This paper aims to illustrate the mission-enhancing capabilities of advanced platform and propulsion technologies[1,2], insofar as small spacecraft are concerned. In the context of challenging deep space missions, it was found that the combination of triple-junction solar cells[1], flexible solar arrays, and gridded ion thrusters[3] operating at high specific impulse (SI) permits total velocity increments of at least 12 km/s to be achieved by an interplanetary spacecraft with a launch mass of less than 200 kg. As an example of possible applications, it was shown that this allows a rendezvous to be achieved with any asteroid selected from a very wide range, commencing from a geostationary transfer orbit (GTO) as an inexpensive auxiliary passenger on an Ariane 5 launch.

The background to this study includes the suggestions, made by JPL in the late 1980s, that lunar scientific missions might be feasible with spacecraft launched from the Shuttle in "Getaway Special Canisters"[4].   To accomplish this, an advanced solar array and a gridded ion thruster operating at a very high SI were employed. Although never flown, this concept was further considered by many research groups, and it was generally concluded that success should be achievable. Two examples studied by the Royal Aerospace Establishment (RAE) at Farnborough were missions to the Kordylewski Clouds[5] to examine the dust particles assumed to be present there and an interplanetary vehicle employing four 10 cm beam diameter ion thrusters[6]. The latter was compatible with the Pegasus launch vehicle. Of course, the viability of the basic idea has now been demonstrated convincingly with ESA's SMART-1 spacecraft[7], albeit using a PPS-1350G Hall-effect thruster[8] operating at a much lower value of SI.

In all such missions the performance of the solar array is critical to the achievement of a significant payload mass. In addition to the power generated per unit mass and per unit area, which can now reach 130 W/kg and 250 W/m² with flexible array technology using triple junction solar cells, the degradation expected during transit through the Earth's radiation belts is of concern.   However, recent advances in solar cell technology have enabled considerable progress to be made in the latter area[9], so that the degradation during transfer from GTO to escape is less than 5%. Other relevant advances in platform technologies include the availability of much improved batteries, attitude and orbit control sensors and actuators with reduced mass, computers and data handling systems which combine lower mass with much increased capabilities, and communications systems offering enhanced performance with reduced mass.

In order to achieve values of SI appropriate for missions of this type, which are of the order of 5000 s and more, gridded ion thrusters are essential[6,10]. While the absolute performance of such devices has almost reached a plateau, significant improvements have been reported in life expectancy, partly through the use of carbon ion extraction grids and also through the attainment of higher values of propellant utilisation efficiency. As regards the overall mass of the ion propulsion system, significant advances are being made in the propellant feed and power conditioning fields. In the former, there have been moves towards microminiaturisation, and in the latter the advent of SiC semi-conductor technology may eventually permit high temperature operation of power conditioning circuits, allowing thermal design constraints to be relaxed[1].

These advances led to the conclusion, as reported in this paper, that a high velocity increment interplanetary mission could be launched as an Ariane 5 auxiliary payload with a mass limit of 200 kg. This launch would be into GTO and the mission would commence with an orbit-raising manoeuvre to escape from the Earth's gravitational field, similar to that demonstrated by SMART-1[7]. This mass enables redundant ion thrusters and a significant payload to be carried, whilst simultaneously allowing the total velocity increment that might be attained to reach at least 12 km/s. Exploratory calculations suggested that a thrust of 30 to 40 mN is appropriate, so the remainder of the analysis was conducted assuming that the spacecraft is equipped with three thrusters each able to provide 17 mN, and that two are operated simultaneously when in Earth orbit and until the output of the array falls to 50% of its initial value as distance from the sun increases. The study included estimates of the mission duration required.

II.   Objectives, Payload and Mission Scenario

A.   Objectives

There has, for many years, been great interest in deep space missions, heightened by the need to understand better the origin and evolution of the solar system, and also by the possibility of finding evidence of past or present life elsewhere. This interest extends to the asteroids and comets orbiting the Sun[11], mainly because they are considered to be remnants of the material from which the solar system was formed. However, a major problem associated with missions to these bodies is the substantial cost involved. This is due largely to the need to provide a very high velocity increment (ΔV) to the spacecraft to escape from the Earth's gravitational field and then to reach the target in a reasonable time. A rendezvous with the target, perhaps to go into orbit around it, adds further to this requirement, which totals many km/s.

Thus the initial objective of this study was to select suitable targets, taking into account the need to minimise launch cost. It was clear that a very large ΔV was mandatory, and preliminary calculations suggested that 12 to 14 km/s might be achieved by a 200 kg spacecraft carrying a reasonable payload. A list of accessible asteroids[12] was examined, together with their orbital parameters and the values of ΔV required to rendezvous with them following Earth escape. These values were between 4.5 and 8 km/s, so are feasible using the spacecraft envisaged in this study. A sample from this comprehensive list is shown in Table 1. Interestingly, further investigation then indicated that it is possible to target up to three such bodies in a single mission. Three asteroids can be visited for a total ΔV of below 10 km/s in at least 14 combinations and all multiple-targets studied require less than 12 km/s.

Table 1. List of possible asteroid targets, with a selection of orbital parameters and values of ΔV.

Asteroid	Class	a (AU)	p (yr)	e	i (deg)	q (AU)	D (km)	ΔV (km/s)
3757 (1982 XB)	S	1.84	2.49	0.446	3.87	1.017	0.5-0.6	7.09
3908 Nyx	V	1.93	2.67	0.459	2.18	1.043	0.7	7.06
4660 Nereus	X or C	1.49	1.82	0.360	1.42	0.953	1.3-1.5	5.37
5797 Bivoj	S	1.89	2.60	0.444	4.19	1.053	0.5	7.45
7341 1991 VK	Sq	1.84	2.50	0.506	5.42	0.909	1.5-1.6	7.99
8014 (1990 MF)		1.75	2.31	0.456	1.86	0.951	0.4-1.2	6.59
8034 (1992 LR)	Q	1.83	2.48	0.410	2.02	1.081	0.8-0.9	6.83
11284 Belenus		1.74	2.30	0.338	1.99	1.153	0.6-2.0	6.71
1977 VA	XC	1.86	2.54	0.394	2.98	1.130	3.6-4.1	7.32
1996 GT		1.64	2.10	0.383	3.40	1.013	0.6-2.0	6.28
1994 CC		1.64	2.09	0.417	4.64	0.955	0.5-1.7	6.88
2001 AE2		1.35	1.57	0.082	1.66	1.239	0.4-1.2	4.69
2001 SK162		1.92	2.67	0.474	1.68	1.012	0.6-2.0	6.85
2001 SW169		1.25	1.39	0.052	3.55	1.184	0.4-1.2	4.58

a = orbital semi-major axis; p = orbital period; e = orbital eccentricity; i = orbital inclination; q = perihelion distance; D = asteroid diameter.

From this examination of possible targets and discussions with relevant experts in this field it was clear that most represent desirable scientific objectives. It was also evident that special expertise and extensive discussion within the science community will be required to select the asteroids giving the best scientific return. Since none of them require a total value of ΔV exceeding 12 km/s, they are all accessible in principle, and there was thus no need to be specific at this stage if this velocity increment can be achieved.

B.   Proposed Payload

An idea of the type of instrument which would be suitable for an asteroid mission can be obtained from the payload carried by the NEAR spacecraft[13], which acquired extensive data from and eventually landed on Eros. Relevant instruments were also carried by DS-1[14] and the Clementine mission to the moon[15]. In the latter case the payload consisted of two star tracker cameras, other cameras operating in the ultra-violet (UV)/visible, near infra-red (IR) and long-wave IR regions, a high resolution camera, and a laser transmitter. The total mass was 7.37 kg and the maximum power consumption 97.3 W. Other relevant missions include ESA's SMART-1 lunar spacecraft[16] and the very challenging Muses-C asteroid sample return mission[17]; the former has now reached lunar orbit[7] and the latter is

nearing its target asteroid[18]. Additional capabilities can be provided by combinations of individual instruments and by the communications systems[16].

A realistic aim for the total mass of the payload is 15 kg, which represents at least 7.5% of the total launch mass. Unusually, the power consumption of the payload is not of critical concern, since the solar array will be sized to accommodate the requirements of two ion thrusters operating simultaneously. Thus, when in orbit around the target, the total output of the array will be available. Taking these factors as the starting point, a possible payload is indicated in Table 2.

Table 2. List of possible payload instruments, with masses and power consumptions

Experiment	Reference	Origin	Mass (kg)	Power (W)
Multispectral camera	13	NEAR	5	10
X-ray spectrometer	16	SMART-1	3	5
Radio science	16	SMART-1	0	0
Magnetometer	13	NEAR	1	1.5
IR spectrometer	16	SMART-1	2	2
Laser rangefinder	17	Muses-C	2	17
Penetrator		-	2	5
Total			**15**	**40.5**

C. Mission Scenario

Since a main objective of this study was to minimise cost, an early decision was to reduce reliance on the performance of the launch vehicle to the greatest possible extent. Normally this policy would imply a launch into low Earth orbit (LEO), followed by a spiral orbit-raising manoeuvre[19] to escape from the Earth's gravitational field. However, the availability of relatively low-cost launches to GTO as auxiliary payloads on Ariane 5 is an attractive alternative[20], and this was eventually adopted as the preferred procedure to be followed.

The other advantages of this approach are illustrated in Table 3, in which the propulsion requirements are compared for launches to GTO and to circular altitudes of 300 and 2000 km.. The results assume that one or two gridded ion thrusters operating with an SI of 4500 s and thrust of 25 mN are employed. The case using a single thruster is presented for comparison purposes.

All three options are clearly viable, although the launches into LEO require the greatest propellant mass, ΔM. Assuming the use of carbon grid technology, the operating times from GTO are acceptable. However, it is likely, for single thruster operation, that a spare might be needed to achieve the total time required, with a switching system to permit a single power conditioning unit (PCU) to be connected to either device. Although an SI of 4500 s was assumed, this is not necessarily the optimum; this can be derived by adding the total mass of the propulsion and power systems as SI is varied. If the range of SI covered is adequately large, a minimum will be found, which represents the optimum conditions. This is because a change in SI at constant thrust alters both the propellant mass required for the mission and the power needed by the thrusters.

**Table 3. Characteristics of the orbit-raising phase of the mission.**

Launch Altitude (km)	ΔV (km/s)	Propellant Mass ΔM (kg)	Thruster On Time (hr)	Time to Escape (days) 1 Thruster	2 Thrusters
300	7.73	32.1	15,746	800	400
2000	6.90	28.9	14,176	683	341
GTO	4.00	17.3	8486	354	177

As an example of the effect of SI, ΔM was calculated as a function of SI for the orbit-raising manoeuvre, assuming the use of T5 gridded ion thrusters[22] operating at 25 mN. The range covered was determined by limiting the ion accelerating potential to 2.3 kV, which is representative of present grid systems[23]. The results (Fig 1) indicate that acceptable values of ΔM are required for all values of SI for a GTO launch, but that there is a mass advantage of about 8 kg in going from 3200 to 5000 s. As expected, ΔM is much larger for the LEO launches. The time required to reach escape velocity, assuming the use of two thrusters simultaneously, is plotted against SI in Fig

4

2. Unfortunately, the use of higher values of SI does not reduce this time, since this is largely determined by the thrust available.
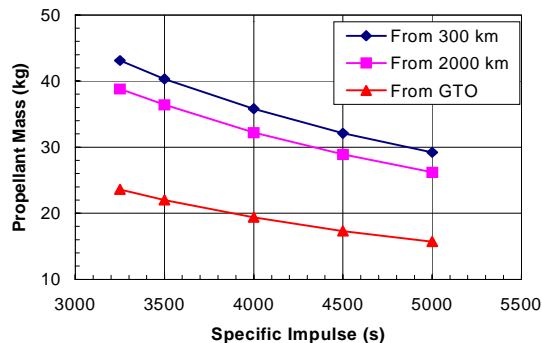
Figure 1. Propellant mass as a function of SI for the orbit-raising phase of the mission.
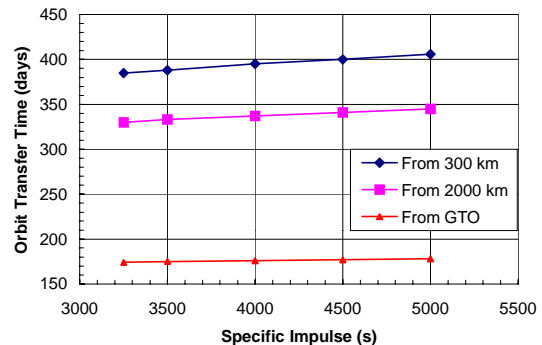
Figure 2. Manoeuvre time as a function of SI for the orbit-raising phase of the mission.

Thus the dominating constraints on this initial phase of the mission are the maximum launch mass of 200 kg and the use of an Ariane 5 launch to GTO. Although target selection must be left to later scientific assessments, it is represented by a worst case ΔV of 8 km/s if only a single asteroid is to be visited. To this must be added the 4 km/s needed for Earth escape, giving a total of 12 km/s. It is proposed that the orbit-raising phase be based on the SMART-1 mission[7,16]. However, thrusting over a wide orbital angle about the apogee to raise the perigee to geostationary altitude would seem to be the optimum initial procedure, followed by continuous thrusting to achieve escape, taking into account, in estimates of the power available, the solar array degradation due to the Earth's radiation environment. Attitude control would be provided by active thrust vectoring, aided by momentum wheels, with momentum dumping by use of auxiliary thrusters, which may be hollow cathode arcjets (HCAs)[21].

The orbit-raising manoeuvre will be followed by the interplanetary trajectory, represented by the ΔV required and the maximum distance from the Sun. Thrusting with the ion propulsion system (IPS) to maximum velocity (to minimise trip time) will then be followed by a retardation phase, again using the IPS, with the aim of a rendezvous with the target. Depending upon the target, various coast phases might be introduced. The ΔV required is between 4.6 and 8.0 km/s, giving a total of 8.6 to 12.0 km/s, including the initial orbit-raising manoeuvre.

Bearing in mind the low gravitational force exerted by all likely targets, the thrust required for capture into orbit should be well within the capabilities of the IPS. A more significant challenge involves terminal navigation, since the target will almost certainly have a low albedo. It may therefore be difficult to acquire it visually at a large distance, so a very slow approach, with the possibility of needing to thrust perpendicular to the velocity vector, may be necessary. However, the value of ΔV required for this and for maintaining the orbital parameters around the target is negligible compared to the maximum of 12 km/s quoted above.

III. Spacecraft Optimisation

D. Basic Mass Budget

Many of the components and systems required to construct this spacecraft are available commercially and are well-documented[1,2,9,24]. They include several recent developments which have resulted in substantial mass savings; examples include Li-ion batteries, advanced computers, and miniature star trackers, attitude control actuators and sensors. In formulating a mass budget for the proposed spacecraft, full advantage has been taken of these new technologies. However, the potential gains provided by miniature propellant feed system components and SiC electronics technology[1] have not been included, since their implementation is still some way in the future.

The mass budget presented below in Table 4 does not include the dominant parts of the power system, which consist of the solar array and the PCUs for the ion thrusters, because the mass of these will vary considerably with SI. Similarly, the propellant and associated tankage are not listed for the same reason. The thrusters have been included, since their mass can be deduced from that of the T5 ion engine[22] without significant errors; in this it was assumed that the mission would require two thrusters with their PCUs to be operating while sufficient power is

The 29th International Electric Propulsion Conference, Princeton University,
October 31 – November 4, 2005

being generated by the solar array. A third is needed for redundancy, thereby also requiring a switching system to allow either PCU to power this device.

Another notable parameter missing from Table 4 is the structure mass. This was assumed to be 12% of the spacecraft wet mass, so was calculated after all other items had been included. Care was taken to ensure that it was adjusted as appropriate as the propellant load changed with SI. The tank mass was assumed to be 10% of the propellant load, which is a pessimistic value, since the Deep Space 1 spacecraft's tank, which was designed many years ago, had a mass of 9.4% of the propellant which it contained[25].

Table 4. Preliminary basic mass budget, excluding power system, propellant, tankage and structure.

ITEM	ESTIMATED MASS (kg)
Payload*	15.0
Pressure regulator system (redundant)	3.0
Ion thrusters (3)	4.8
Gimbal mounts (3)	4.5
Switch unit	1.0
Flow control units (3)	1.5
IPS harness	2.0
IPS pipework and fittings	1.0
Array rotation mechanism (redundant)	2.5
Array electronics (redundant)	3.6
Battery (not for IPS use)**	3.4
Data handling unit (computer and memory)	2.4
Communications system	7.0
Sun and Earth sensors	1.0
Star tracker (redundant)	1.5
GPS system (for orbit-raising phase)	1.0
ACS thrusters	2.0
ACS power supplies and switches	1.3
Control moment gyros (CMGs)	2.0
Launch adaptor	6.0
Thermal control	6.0
Harness	2.0
TOTAL	**74.5**

*   The payload mass is a defined number and any mass over-run would normally be dealt with by reducing the scope of the mission, as necessary.
** The battery capacity and thus its mass is somewhat arbitrary; it is required to power the platform systems during eclipse while in the orbit-raising phase and during any subsequent emergency situations.

E. The Solar Array

In all studies of solar-powered interplanetary missions, the performance of the solar array is critical to the achievement of a significant payload mass. In addition to the power generated per unit mass and per unit area, which can now reach 130 W/kg and 250 W/m², the degradation during transit through the Earth's radiation belts is of concern. However, recent progress has enabled the degradation during transfer from GTO to escape to be reduced to less than 5%.

There has been considerable success in improving the performance of solar cells and thus of complete arrays. For example, certain high-eta Si cells have initial efficiencies ranging from 15.5 to 17.3%, depending on whether the cell is optimised for beginning-of-life (BOL) efficiency, radiation resistance or cell mass. The main advantages of these cells over other candidates are that they are lighter, with approximately one third of the mass and less than 50% of the cost.

GaAs/Ge cells, which are available from commercial sources, have a typical BOL efficiency of 19%, with superior radiation resistance compared to Si cells. The temperature coefficients are also better, so that there is less reduction of efficiency with increasing temperature. However, dual and triple junction (TJ) cells are the current state-of-the-art devices, although the former are already being superseded by the latter. Dual junction cells are typically 24 to 25% efficient, and the triple junction types reach 27 to 28% and are forecast to be close to 30% in the next few years. They all have a superior radiation resistance compared to GaAs/Ge technology. These cells have a relatively high operating voltage, which simplifies array construction; they provide 2.2 V, as compared to 0.85 V and 0.45 V for GaAs/Ge and Si, respectively. It was therefore assumed that TJ cells with 28% efficiency are used in the mission discussed in this paper.

Rigid panel arrays are the most common type in use. Carbon-fibre skinned aluminium panels are hinged together and deployed out from the sides of the spacecraft. The mass per unit area is rather high, so a flexible blanket array is more attractive for the present application. This often consists of a reinforced Kapton blanket, supporting the solar cells and their interconnections, which is folded up, concertina fashion, into a box and then deployed using an appropriate boom or mast. In between each fold is a "leaf" of Kapton to protect the cells. An early example of this type was the RAE array[26] used on the Miranda (X4) spacecraft flown in 1974.

The Miranda array, which was only partially populated with active cells, produced 310 W from 7440 2 cm x 2 cm Si cells with an efficiency of 7.7%, and for a mass of 11.8 kg, ie about 26 W/kg. However, for the X5 mission[27] the array was to be fully populated with 14,880 Si cells, giving an output of 561 W for a mass of 47 W/kg. If modern TJ cells are transposed onto this latter array, the resulting performance figures are 2040 W, 131 W/kg, and 268 W/m^2; see Table 5, in which Muses-C data are included for comparison. These improvements are very significant indeed, and it was assumed that an array of this type would be appropriate to this mission.

Table 5. Summary of characteristics of various solar arrays.

Array Type	Cell Type	Efficiency	Power (W)	Mass (kg)	Power/Mass (W/kg)	Power/Area (W/m^2)
Muses-C (end of life data)	TJ	-	2500	47.2	53	236
X4 flexible type	Si	7.7	310	11.8	26	41
Upgraded X4 flexible type	TJ	28	1127	15.6	50	149
X5 flexible type	Si	7.7	561	11.8	47	74
Upgraded X5 flexible type	TJ	28	2040	15.6	131	268

For orbit-raising through the Earth's radiation belts, the radiation dose received by the array is the main design driver. This will depend upon the initial orbit and how quickly the radiation belts can be traversed. Ideally, this transfer requires radiation hard technology and a thick coverglass to shield the cell, thus a TJ type is preferable. For example, the degradation of GaAs/Ge cells using 500 μm coverglasses, flown on the QinetiQ STRV1-b satellite[9] in GTO, is illustrated in Fig 3. This predicts a degradation of below 7% for a transfer from GTO to Earth escape in 1 year, and it should be noted that TJ cells will provide a better performance than this.

F. The Thruster PCU

Another variable in assessing total spacecraft mass is the PCU, two of which are required for this mission. This device[28] converts the solar array power into the controlled voltages and currents required by the thruster and, in many cases, also controls the complete thruster system, including the propellant feed system. It also provides the essential interface with the spacecraft's data handling and telemetry
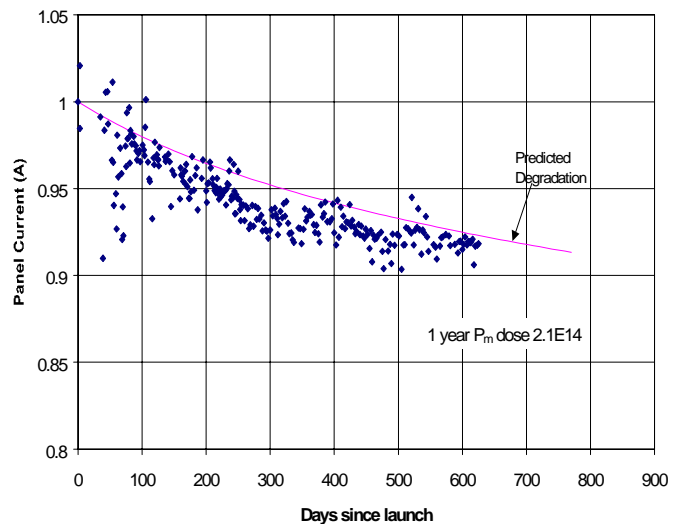

Figure 3. Degradation of STRV-1b GaAs/Ge solar panel in GTO.

systems. The mass of this unit clearly depends upon the functions which it undertakes, but the main variable is the output power, which changes rapidly with SI.

It is not possible to calculate theoretically the mass of a typical PCU, but sufficient data have been published from a wide variety of thruster development programmes to permit a broad guide to be produced, covering the power range to about 2 kW. This guide is shown in graphical form in Fig 4. It does not include the advances anticipated in the future from the use of electronics based on SiC technology[1], although a mass reduction of the order of 50% has been predicted. This will come largely from a major simplification of the thermal control problems which beset high power PCU designs[28], as well as from efficiency increases.

The PCU is not fully efficient, so this factor has to be taken into account in assessing the power output required of the solar array. Modern PCUs operate with efficiencies in the 90-95% region, but, to provide some margin, it was assumed here that an efficiency of 88% would be achieved.
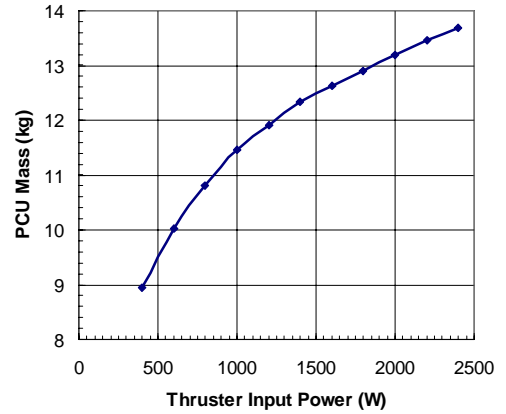
Figure 4. PCU mass as a function of thruster input power.

G. Optimisation of SI

The power required to be produced by the solar array is used for two purposes; the platform systems, including the payload, and the IPS, with the latter dominating. It was assumed that 300 W would be a generous allocation for the platform systems and payload, and that the power to the IPS would be determined solely by the SI required, at constant thrust. As mentioned earlier, preliminary assessments were based on the need to provide the full 12 km/s, and that the time to reach the target, assumed to be at a distance of 2 AU, should not be more than 3 years. After including margins, this led to the conclusion that the total thrust should be in the range 30 to 40 mN, so it was decided that each thruster should produce 17 mN. The power required at this thrust was then calculated as a function of SI, assuming the use of a Kaufman-type thruster[22] with the configuration shown schematically in Fig 5.

To evaluate the total power required, the procedure adopted was as follows. The total propellant flow to the thruster, $\dot{m}_T$, was first derived from the definition of SI,

$$I_{sp} = \frac{T}{\dot{m}_T g_o} \tag{1}$$

where I_{sp} is the SI, T is the thrust, and g_o is the acceleration due to gravity at sea level. The flow through the neutraliser cathode, assumed to be 0.036 mg/s[22], was then subtracted from $\dot{m}_T$ to give the flowrate into the discharge chamber, $\dot{m}_D$. This enters the discharge via the main flow path and through the hollow cathode, as indicated in Fig 5.

The next step was to calculate the beam current, I_B, at 17 mN thrust, assuming that the propellant utilisation efficiency, η_m, is 0.85, which is typical of modern gridded thrusters. For this, the following equation was used:

$$I_B = \frac{e \dot{m}_D \eta_m}{m_i} \tag{2}$$

where e is the charge on an electron and m_i is the ion mass. This value then enabled the typical discharge power, P_D, to be determined, using experimental data acquired in extensive throttling tests of the T5 ion thruster, covering the thrust range 0.3 mN to 71 mN[23,29] (see Fig 6). This power included the main anode-cathode discharge, the keeper-cathode discharge and the power dissipated in the solenoids.

To calculate the total power input to the thruster it was then necessary to determine the beam accelerating potential, V_B, since the power contained within the beam is $P_B = I_B V_B$. Knowing I_B from Equ 2, V_B was found from
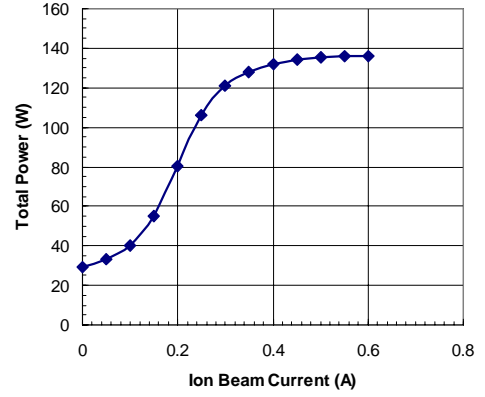
$$T = I_B \left(\frac{2 V_B m_i}{e} \right)^{1/2} \tag{3}$$

The total input power, P_T, is then

$$P_T = P_D + P_B + P_N \tag{4}$$
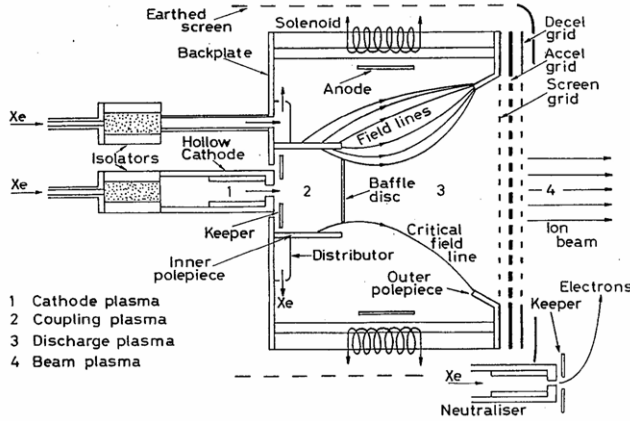
Figure 5. Schematic Diagram of a Kaufman-type ion thruster.

Figure 6. Total discharge power as a function of beam current.

where P_N is the power consumed by the neutraliser discharge, which was assumed to be 16 W from T5 experience. This value was then divided by the power conditioning efficiency, assumed to be 0.88, to give the input power into a single thruster system. The total power required from the array at end of life was then equal to double this, to account for the operation of two thrusters simultaneously, plus the 300 W assumed to be required by the platform and payload. To obtain the beginning of life output, this result was increased by 5% to account for array degradation caused by radiation, mainly in the orbit-raising phase of the mission. This final value then gave the mass of the flexible array, assuming a power-to-mass ratio of 130 W/kg (see Table 5).

Finally, the array mass was added to the basic spacecraft mass given in Table 4. This total was then multiplied by 1.12 to account for the associated spacecraft structure, assumed to be 12% of the mass to be carried. This aggregate mass, designated M_b, included the complete spacecraft apart from the propellant, its tank and the additional structure required to accommodate it.

In the optimisation process, the next step was to evaluate the propellant mass, ΔM, required, which was expected to vary strongly with SI. This was done by using the "rocket equation"[1], which relates the total spacecraft mass before the mission, M_i, and that at the end, M_f, to the SI and to ΔV. This can be expressed as

$$M_f = M_i \exp\left(\frac{-\Delta V}{I_{sp}g_o}\right) \tag{5}$$

where $(M_i - M_f) = \Delta M$. To include the tank mass and the associated structure, ΔM was increased by the factors α_t and α_s. These were assumed to be 0.1 and 0.12, respectively. The total mass associated with the propellant is then

$$\Delta M_t = (1 + \alpha_t)(1 + \alpha_s)\Delta M \tag{6}$$

Thus

$$M_i = M_b + \Delta M_t \quad \text{and} \quad M_f = M_b + \Delta M_t - \Delta M \tag{7}$$

but noting that M_f, M_i and ΔM are all unknowns at this stage. However, by re-arranging Equs 5, 6 and 7, with $K = M_f/M_i$,

$$\Delta M = M_b \frac{(1 - K)}{(1 + \alpha_t)(1 + \alpha_s)(K - 1) + 1} \tag{8}$$

which permits all the unknown masses to be determined.

The optimisation results, which cover a range of SI from 2500 to 14,000 s, are shown in Fig 7. It can be seen that, as expected, the mass associated with the propellant decreases rapidly as SI is increased, but that the power system mass increases. The total of these two has a minimum at about 8000 s, which is thus the optimum SI if launch mass is the criterion upon which a decision is to be made. It is interesting to note that, owing to the different shapes of the power and propellant system curves, the optimum is not at their point of intersection, as is sometimes assumed.

In many mission analyses, the initial mass is critical, because the cost of the launch is very large and can dominate the economics of the mission. If, however, a relatively low-cost auxiliary launch is possible, as in the case considered here, the dry mass of the spacecraft becomes much more significant. This is because the development and manufacturing costs are determined largely by this mass, since the propellant is relatively inexpensive. In particular, the solar array is a very costly item, so the size of this should be minimised insofar as this is possible. To illustrate the difference between these two criteria, the launch and dry masses are plotted against SI in Fig 8, from which it is clear that the optimum SI is much reduced if dry mass is the most important factor to be considered; it is then about 4300 s.
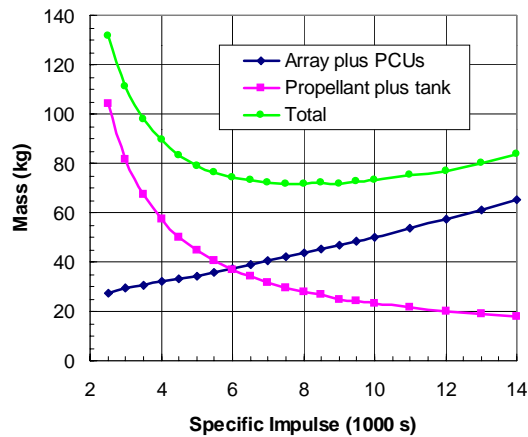
Figure 7. Masses of power and propellant systems, and their total, as functions of SI
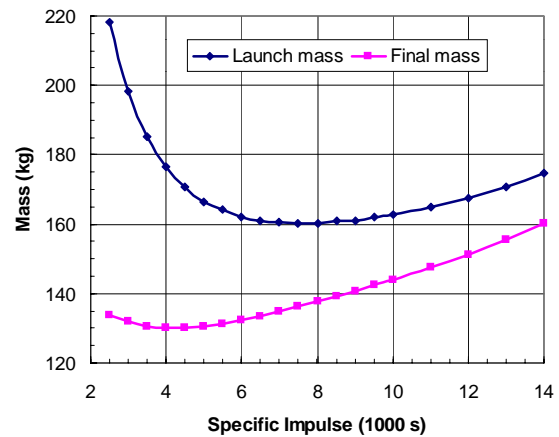
Figure 8. Launch and dry spacecraft masses as functions of SI.

In reality, a more complex analysis in which actual cost is the dominant criterion will give a third optimum, which will be located between the two described above. However, in the case of a low cost launch, the development and production costs are likely to be the most significant so, in this study, a value only slightly higher than that based on the dry mass was adopted, 5300 s. This was influenced by the maximum value of V_B currently used in gridded ion thrusters, which is about 2.5 kV[23,30].

H. Spacecraft and Mission Parameters

Taking achievable published masses for the various spacecraft systems, as indicated in Table 4, and assuming a payload mass of 15 kg, Fig 8 suggests that the launch mass with an SI of 5300 s will be 165 kg. If a 20% contingency of 33 kg is added, as is common practice, the total remains below 200 kg, which was the original objective. It is notable that the selection of 5300 s, when compared to 4800 s, provides a slight reduction of about 4 kg in launch mass, for an increase in dry mass of less than 1 kg. From Fig 7, the propellant system mass required for the mission, assuming the full ΔV of 12 km/s, is a modest 42 kg, of which 34 kg is xenon.

With these parameters, as shown below the beginning-of-life power required is well below 2 kW; it is 1808 W, including a contingency of 10%. Thus a smaller version of the upgraded X4/X5 solar array discussed earlier and using TJ cells (see Table 5) will be fully adequate for the mission. Assuming an unchanged width of 0.91 m, each wing will have a span of 3.71 m. The total mass will be about 13.9 kg.

It is envisaged that the spacecraft configuration will be conventional, with a central body containing all housekeeping systems, the ion thrusters, and a large high gain antenna for communicating with the Earth. The wings of the array will protrude symmetrically on either side of this body. Either a single propellant tank will be mounted with the centre of mass (CoM) of the vehicle close to its geometric centre, to avoid changes of the CoM as propellant is used, or multiple inter-connected tanks will be employed, placed symmetrically about the CoM. An alternative might be a toroidal tank surrounding the CoM.

In all design options, the resultant thrust of the operating engines must pass through the CoM; this is ensured by mounting the thrusters on gimbal platforms, which can also be employed to provide attitude control during thrusting. Since thrusting will be required for almost the entire mission, this latter feature will reduce the amount of attitude control propellant to minimum. Of course, thrust vectoring will provide attitude control about only two axes. As indicated in Table 4, CMGs will be used in the roll axis, with HCAs[21] employed for occasional de-saturation.

With the selected thruster parameters, the time to escape from the Earth's gravitational field is about 210 days, assuming continuous thrusting. The total mission time, without thrust-off cruise periods, is 800 days, assuming that the asteroid rendezvous requires the full 12 km/s and that it occurs at a distance from the sun of 2 AU.

IV. Thruster Design

The design of this thruster was based on the physical data and scaling relationships so successfully employed in the T5[10,22] and UK-25[30] devices. These, in turn, rely heavily on an important characteristic of the Kaufman-type thruster, which is that its different plasma regions (Fig 5) can be treated separately from each other to a first approximation, and also that the ion extraction and acceleration process can be analysed independently.

The starting point was the grid system. It was decided that this should be essentially identical in its geometry to that of the T5 thruster. However, it was assumed that molybdenum grids would be replaced by carbon to improve resistance to damage by sputtering, thereby yielding a longer life at lower cost.

Once the configuration of the grids was established, the discharge chamber was scaled as in the previous designs[30-32], using the relationships established at that time. As mentioned above, this process relied upon being able to treat the different regions of the thruster (Fig 5) independently. Special care was necessary, however, in dealing with the interfaces between the cathode and the coupling plasma, and between the latter and the main discharge region.

I. Ion Extraction and Acceleration

From Equ 3, T will increase with V_B, but decrease if m_i is reduced. Compensation for this can be obtained by extracting a larger I_B, which requires a higher plasma density in the discharge chamber and thus a greater discharge power. The limit is the ability of the grids to pass this increased current. This is determined by their perveance, which can be defined[31] as

$$\frac{I_B}{V_T^{3/2}} = \frac{4\varepsilon_o}{9}\left(\frac{2e}{m_i}\right)^{1/2}\frac{AT_g}{d^2} \tag{9}$$

In this expression, $V_T = \left(V_B + |V_{ac}|\right)$ is the total ion accelerating potential, where V_{ac} is the accel grid potential, ε_o is the dielectric constant of free space, d is the ion acceleration distance, A is the area of the grids, and T_g is the effective transparency of the screen grid. This leads to the definition of a perveance parameter, P_g, which is

$$P_g = \frac{I_B m_i^{1/2} d^2}{AT_g} = \frac{4\varepsilon_o\sqrt{2e}}{9}V_T^{3/2} \tag{10}$$

As can be seen in Fig 9, a logarithmic plot of P_g against V_T is linear; here, for historical reasons, I_B is in amps, m_i is in AMU, d is in mm, and A is in m^2. Experimental points from the T5[10,22,23] and UK-25[30] Kaufman-type thrusters were used to provide the indicated trends and are consistent with the expected 3/2 power law.

The data in Fig 9 fall on two lines, labelled "peak performance" and "Artemis conditions". The former represents the maximum perveance case, where lifetime is likely to be limited. The "Artemis" line applies to the conditions required for long life, as specified for the T5 thruster for operational use on the Artemis communications satellite[33], for which a lifetime of close to 15,000 hours was required. Thus the latter was most appropriate to a long duration interplanetary mission and, with $V_B = 2.5$ kV and $V_{ac} = -250$ V, $P_g \sim 1100$.

With these parameters fixed, together with T and I_{sp}, $\dot{m}_T$ and $\dot{m}_D$ were obtained from Equ 1, I_B from Equ 2, and the various significant power levels were calculated as indicated previously. With d determined by previous practice, the value of P_g taken from the lower line in Fig 9
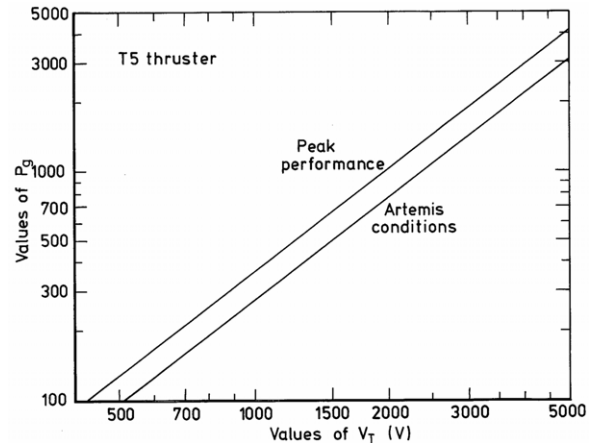

Figure 9. Perveance factor as a function of total ion accelerating potential (derived from T5 thruster data).

The 29th International Electric Propulsion Conference, Princeton University,
October 31 – November 4, 2005

yielded the required grid area, under the assumption that T_g was unchanged. This completed the definition of the grid system, the active diameter of which is 5 cm. Taking into account the need to screen the outer region of the discharge chamber, where the plasma density profile falls away steeply, and to accommodate the anode, the discharge chamber diameter was set at 8 cm. This screening provision is necessary because very wide variations of ion current density are not compatible with long life, using the desirable simple grid geometrical design. Finally, it was assumed in this analysis that the plasma density profile in the new thruster would be identical to that in the existing devices[34].

J. The Discharge Chamber

Following Refs 31 and 35, to maintain the same ion production per primary electron in the discharge chamber as in the T5 and UK-25 devices, and hence the same ionisation efficiency, the product BR should be kept constant when scaling a thruster. Here, B is a measure of the magnetic flux density and R is the dominant dimension, the radius of the ion beam. Since B varies throughout the chamber, this implies that its geometrical distribution must be unchanged, so the configuration of the magnetic circuit was retained in all essential features in the new design. There was no need to quantify B, because the appropriate value to satisfy all conditions can be set by adjusting the current through the solenoids (Fig 5).

When BR is fixed in this way, the proportion of the ions which diffuses longitudinally towards the grids is independent of R, provided that the aspect ratio R/L is not changed. Thus the length L, which is defined as the distance from the upstream side of the screen grid (Fig 5) to the downstream face of the baffle disc, is inversely proportional to the radius. This relationship, which ensures that the relative flux of ions reaching the grid system is independent of thruster size, was used to calculate L from the T5 and UK-25 dimensions; it is 3.2 cm.

This scaling aimed to ensure that the primary electron containment time in the new thruster is at least as great as in the previous designs. To achieve this, another criterion was that the anode must not intersect any magnetic field line originating from the tip or inner surface of the inner polepiece, otherwise primary electrons can be lost before they suffer ionising collisions. To do this, the longitudinal position of the anode was scaled linearly from the T5 thruster, and its internal diameter was selected to be greater than that of the beam by at least the same amount as in the earlier device; 1 cm was selected in this case, giving an anode internal diameter of 7 cm.

The ion production rate in the discharge chamber can be described as a current I^+. The ionisation efficiency may then be defined as I^+ / I^-, where I^- is the primary electron current. This efficiency depends upon many factors, but most are held constant in the scaling process. One which remains a variable is the ionisation cross section, which depends upon the energy of the primary electrons. This is a function of the anode potential, V_A, which can be varied as necessary to achieve the required performance, provided that it does not exceed a limit determined by the rate of sputter erosion in the discharge chamber[36]. A nominal value of 38 V was selected to give a compromise between discharge chamber efficiency and lifetime.

Previous experience suggests that I^+ / I^- is about 0.5, provided that the primary electrons have adequate energy. Similarly, it was found by experiment that the ion flux in the downstream direction provides a beam current given by $I_B \approx 0.23 I^-$. Thus

$$I_A = I^- + I^+ \approx 1.5 I^- \approx 6.5 I_B \tag{11}$$

The anode length was then selected on the basis of maintaining the same current density as within the T5 thruster operating under nominal conditions. To do this, I_A was required; it was obtained from the above empirical relationship.

K. Cathode and Coupling Plasma

The primary electrons originate from the hollow cathode, which must therefore be capable of providing the necessary current in a manner consistent with long life. The cathode designed for the T5 thruster[37] is suitable in this respect and therefore forms the basis of the device to be fitted to the new device. Although the mode changes seen in cathode discharges in a diode configuration[37] are not so evident when in a thruster, it was important to avoid noisy conditions, since these can lead to thruster instability. Thus an important criterion in selecting the cathode flow rate, $\dot{m}_c$, was that it should be sufficient for steady, quiet operation. For the T5 cathode, this was about 0.1 mg/s. It was to decided to retain this value.

In scaling the inner polepiece and baffle disc, a detailed understanding of the mechanisms responsible for the extraction and acceleration of the primary electrons from the coupling plasma is implied. Fortunately, this was accomplished[32] in the past in preparation for the design of the T5 thruster. With this foundation, all that was needed

was to ensure that the current density of primary electrons passing through the annular gap between the baffle disc and the inner polepiece (Fig 5) was unchanged. Since I_B / I^- is a constant, linear scaling with R was appropriate to first order. However, this assumed that the conditions in the coupling plasma were consistent with the primary electron current required. Calculations to ensure that this was so were based on the treatment presented in Ref 32, and involved a simple estimate of the flux of electrons diffusing towards the annular gap, relative to the situation in the T5 thruster. This took into account the cathode flow rate in the new thruster and the reduced magnetic field, as well as the dimensional changes.

If the potential through which the primary electrons are accelerated is $\Delta(V_p - p_e)$, where V_p is the plasma potential and p_e is the electron pressure

$$\Delta(V_p - p_e) \propto \frac{j_p B T_e^{1/2}}{n_e^{3/2}} \tag{12}$$

where n_e and T_e are the electron number density and temperature, respectively, and j_p is the current density perpendicular to the magnetic field lines in this region and flowing towards the annular gap.

In practice, $\Delta(V_p - p_e) \approx (V_A - V_k)$, where V_k is the potential of the keeper electrode. Thus, rearranging the above expression, using subscript "o" to denote the T5 thruster and "n" the new device, and recalling that $B_n / B_o = R_o / R_n$

$$j_{pn} \approx j_{po} \frac{(V_A - V_k)_n}{(V_A - V_k)_o} \frac{R_n}{R_o} \left(\frac{n_{en}}{n_{eo}}\right)^{3/2} \tag{13}$$

Since T_e is 1 eV or less, there will be very little ionisation within the coupling plasma. So, assuming that recombination can also be ignored, the value of n_e at the annular gap will be linearly dependent upon $\dot{m}_c$, and inversely proportional to the distance, s, from the cathode orifice. Thus, Equ 13 becomes

$$j_{pn} \approx j_{po} \frac{(V_A - V_k)_n}{(V_A - V_k)_o} \frac{R_n}{R_o} \left(\frac{\dot{m}_{cn}}{\dot{m}_{co}}\right)^{3/2} \left(\frac{s_o}{s_n}\right)^3 \tag{14}$$

As V_k is about 12 V in each case, and knowing that $j_{po} = 0.76$ A/cm^2 for the T5 thruster at 25 mN thrust, this expression gave $j_{pn} \approx 1.07$ A/cm^2 for the new design. This represents the largest primary electron flux that can be extracted through the annular gap, and a maximum electron current of 1.8 A. The actual value required at 17 mN thrust is 1.2 A, thereby providing a satisfactory margin. Should this margin be inadequate in practice, it can always be increased by employing a larger cathode flow rate and/or a higher keeper current.

L. Performance Assessment
The analysis reported above led to the following set of performance parameters for this thruster:

Beam diameter	5 cm
Discharge chamber diameter	8 cm
Specific impulse	5300 s
Thrust	17 mN
Input power	521 W
Total propellant flow rate	0.323 mg/s
Electrical efficiency	85.7%
Propellant utilisation efficiency	85%
Total efficiency	72.8%
Power-to-thrust ratio	31.2 W/mN

V. Conclusions

It has been shown that a small spacecraft, with a launch mass of less than 200 kg, including a contingency of 20%, can provide a total velocity increment of 12 km/s, thereby allowing a scientifically useful payload to be delivered to any one of a wide variety of asteroids. Such a capability will enable the spacecraft to rendezvous with the asteroid, then be placed in an orbit around it, so that scientific data can be collected over a long period of time.

However, a challenging mission of this type can be achieved within such a low mass budget only by employing a propulsion system able to provide a very high value of specific impulse; this implies the use of gridded ion thrusters. In addition, an advanced solar array with a power-to-mass ratio exceeding 100 W/kg is also mandatory. Such an array can be produced by re-using the flexible substrate design flight tested successfully in the 1970s on the X4 satellite, but populated with modern triple junction solar cells.

The envisaged mission aims to minimise cost by launching as an auxiliary payload, on an Ariane 5 rocket, into a geostationary transfer orbit. The ion thrusters will then be used to expand this orbit until escape from the Earth's gravitational field is achieved. It was assumed that two thrusters will be operated simultaneously at a total thrust of 34 mN, with a third device provided for redundancy. Such a process has already been ably demonstrated by ESA's SMART-1 spacecraft, using a single Hall-effect thruster. The mission would then enter the interplanetary trajectory phase.

An optimisation process demonstrated that two different results are found, depending on whether the aim is to minimise launch mass, and thus launch cost, or to reduce the cost of the hardware to be flown. The latter is accomplished by minimising the dry mass of the vehicle. In the case of a relatively low cost launch, concentration on the hardware cost is probably preferred, giving an optimum SI in the case studied of about 4300 s. To minimise launch mass, the optimum is much higher, at 7700 s. However, to complete the analysis it was decided to adopt a moderate increase on the former value, to 5300 s. This provides a useful decrease in propellant mass for an increase in dry mass of less than 1 kg, and is within the capabilities of present ion thruster designs.

The final stage of the study was to produce a conceptual design of a thruster suitable for this mission. Based on previous experience gained with the T5 and UK-25 thrusters, it was found that the required 17 mN at 5300 s SI can be provided by a device with a beam diameter of 5 cm, a discharge chamber diameter of 8 cm, and a modest beam current of only 0.18 A. The input power is 530 W and the electrical and propellant utilisation efficiencies are both about 85%, giving a total efficiency of nearly 73%.

References

[1]Clark, S. D., Fearn, D. G. and Marchandise, F., "A Study into the Techniques for Miniaturised Electric Propulsion Systems, and Mission Categories, for Small Spacecraft", IEPC Paper 03-216, March 2003.

[2]Blott, R. J., Wells, N. S. and Eves, J., "The STRV 1 Microsatellite Series: the Rapid, Low Cost Route for Innovative in Orbit Technology Testing", *J Brit Interplan Soc,* Vol 51, No 10, pp 387-400, 1998.

[3]Martin, A. R., Moulford, W. E. F. L., and Fearn, D. G., "Low-Cost Interplanetary Missions Using Electric Propulsion", *J Brit Interplan Soc,* Vol 49, pp 447-454, 1996.

[4]Nock K. T., Aston, G, Salazar, R. P. and Stella, P. M., "Lunar Get-Away Special (GAS) Spacecraft", AIAA Paper 87-1051, May 1987.

[5]Ryden, K. A., Herrington, P. G. and Wallace, N. C., "A Case Study of a Mission to the Kordylewski Clouds Using Ion Propulsion", IEPC Paper 88-068, October 1988.

[6]Fearn, D. G. and Martin, A. R., "The Promise of Electric Propulsion for Low-Cost Interplanetary Missions", *Proc Conf on "Low cost planetary missions",* Johns Hopkins University, Maryland, 12-15 April 1994; *Acta Astronautica*, Vol 35, pp 615-624, 1995.

[7]de Cara, D. M. and Estublier, D., "SMART-1; an Analysis of Flight Data", IAF Paper IAC-04-S.4.02, October 2004.

[8]Dumazert, P., Marchandise, F., Prioul, M., Darnon, F. and Jolivet, L., "PPS 1350-G Qualification Status", IEPC Paper 03-270, March 2003.

[9]Blott, R. J., Wells, N. S. and Eves, J., "The STRV1 Microsatellite Series: Exploiting the Geosynchronous Transfer Orbit", *Acta Astronautica,* Vol 41, No 4-10, pp 481-491, Aug-Nov 1997.

[10]Fearn, D. G., Martin, A. R. and Smith, P. "Ion Propulsion Development in the UK", IAF Paper IAF-93-S.5.490, October 1993.

[11]Taylor, R. L. S. and Fearn, D. G., "After Eros – Future Multiple-Target Dedicated Asteroid Missions", *J Brit Interplan Soc*, Vol 56, No 1/2, pp 2-32, January/February 2003.

[12]Parkinson, R. C., Astrium UK Ltd, Private Communication.

[13]Santo, A. G., Lee, S. C. and Gold, R. E., "NEAR Spacecraft and Instrumentation", *J of the Aeronautical Sciences,* Vol 43, No 4, pp 373-397, October-December 1995.

[14]Rayman, M. D., Varghese, P., Lehman, D. H. and Livesay, L. L., "Results from the Deep Space 1 Technology Validation Mission", IAF Paper IAA-99-IAA.11.2.01, October 1999.

[15]Rustan, P. L., "Clementine: Mining New Uses for SDI Technology", *Aerospace America*, Vol 32, No 1, p 38, 1994.

[16]Racca, G. D., Foing, B. H. and Rathsman, P., "An Overview on the Status of the SMART-1 Mission", IAF Paper IAA-99-IAA.11.2.09, October 1999.

[17]Kawaguchi, J. and Uesugi, K. T. K., "Technology Development Status of the Muses-C Sample and Return Project", IAF Paper IAF-99-IAA.11.2.02, October 1999.

[18]Kuninaka, H., Shimizu, Y., Yamada, T., Funaki, I. and Nishiyama, K., "Flight Report During Two Years on Hayabusa Explorer Propelled by Microwave Discharge Ion Engines", AIAA Paper 2005-3673, July 2005.

[19]Fearn, D. G., "The Use of Ion Thrusters for Orbit-Raising", *J Brit Interplan Soc*, Vol 33, No 4, pp 129-137, April 1980.

[20]Ravet, L. and Durand, J., "The Ariane 5 Launcher Improvements After 5 Years of Operation", IAF Paper IAF-01-V.1.03, October 2001.

[21]Gessini, P., Gabriel, S. and Fearn, D., "The T6 Hollow Cathode as a Microthruster", AIAA Paper 2005-4078, July 2005.

[22]Fearn, D. G. and Smith, P., "A Review of UK Ion Propulsion - a Maturing Technology", IAF Paper IAF-98-S.4.01, September/October 1998.

[23]Martin, A. R. and Latham, P. M., "High Thrust Operation of the UK-10 Rare Gas Ion Thruster (T4A)", IEPC Paper 88-062, October 1988.

[24]Clark, S. D. and Fearn, D. G., "The Impact of Advanced Platform and Ion Propulsion Technologies on Small, Low-Cost Interplanetary Spacecraft", *Proc 5th IAA Internat Conf on "Low-Cost Planetary Missions",* ESTEC, Noordwijk, Holland, 24-26 September 2003; ESA SP-542.

[25]Brophy, J R, "Ion Propulsion System Design for the Comet Nucleus Sample Return, Mission", AIAA Paper 2000-3414, July 2000.

[26]Day, B. P. and Treble, F. C., "The Ion Engine and Large Solar Array for the X-5 Spacecraft", RAE Farnborough Technical Report TR 68191, Aug 1968.

[27]Fearn, D. G., "Orbit-Raising, Past and Present – the X-Series of Spacecraft and Artemis", IEPC Paper 2005-227, October/November 2005.

[28]Lovell, M., "The UK-10 Power Conditioning and Control Equipment", AIAA Paper 90-2631, 1990.

[29]Fearn, D. G., "A Study of the Throttling of the T5 Ion Thruster", AIAA Paper 96-3288, July 1996.

[30]Latham, P. M., Martin, A. R. and Bond, A., "Design, Manufacture and Performance of the UK-25 Engineering Model Thruster", AIAA Paper 90-2541, July 1990.

[31]Harbour, P. J., Wells, A. A., Harrison, M. F. A. and White, B. M., "Physical Processes Affecting the Design and Performance of Ion Thrusters with Particular Reference to the RAE/Culham T4 Thruster", AIAA Paper 73-1112, 1973.

[32]Wells, A. A., "Current Flow Across a Plasma "Double Layer" in a Hollow Cathode Ion Thruster", AIAA Paper 72-418, April 1972.

[33]Oppenhaeuser, G., van Holtz, L. and Bird, A., "The Artemis Mission – ESA's Latest Communication Satellite", IAF Paper IAF-01-M.1.08, October 2001.

[34]Bond, R. A. and Latham, P. M., "Ion Thruster Extraction Grid Design and Erosion Modelling Using Computer Simulation", AIAA Paper 95-2923, July 1995.

[35]Wells, A. A., Harrison, M. F. A., White, B. M. and Harbour, P. J., "Laws for Scaling Electron Bombardment Thrusters", *Proc IEE Conf on "Electric Propulsion of Space Vehicles",* Culham Laboratory, UK, April 1973. IEE Conf Publication 100, pp 250-257, 1973.

[36]Fearn, D. G., "Ion Thruster Lifetime Limitations Imposed by Sputtering Processes", IEPC Paper 93-177, September 1993.

[37]Fearn, D. G., Singfield, A., Wallace, N. C., Gair, S. A. and Harris, P. T., "The Operation of Ion Thruster Hollow Cathodes Using Rare Gas Propellants", AIAA Paper 90-2584, July 1990.